ELSEVIER

Contents lists available at ScienceDirect

Medical Engineering and Physics

journal homepage: www.elsevier.com/locate/medengphy



Technical note

Effect of composite coating on insertion mechanics of needle structure in soft materials



Kavi I Patel, Long Zhu, Fei Ren, Parsaoran Hutapea

Department of Mechanical Engineering, Temple University, Philadelphia, PA 19122, United States

ARTICLE INFO

Keywords:
Needle insertion mechanics
Friction force
Polymer-coated needle
Polydopamine
Polytetrafluoroethylene
Activated Carbon

ABSTRACT

This research aims to study the effect of a composite coating comprised of polydopamine (PDA), polytetra-fluoroethylene (PTFE), and activated Carbon on the insertion mechanics of surgical needles in tissues i.e., polyvinyl chloride (PVC) tissue phantom and bovine kidney. A needle insertion and extraction test system was designed and constructed to measure the insertion and extraction forces. It was found that the composite coating on the needle surface decreases the maximum average insertion and extraction forces by 62% and 64%, respectively, when tested in PVC tissue phantom and by 49% and 30%, respectively, in bovine kidney tissue. Additionally, an Atomic Force Microscope study was performed to characterize the surface properties of the coated needles. It was found that the composite coating reduced the friction force on the needle surface by 65.7%. The decrease in these forces is critical in minimizing tissue damage and decreasing needle path deviation or deflection during percutaneous procedures.

1. Introduction

Percutaneous procedures such as biopsy, brachytherapy, thermal ablation, and drug delivery utilize surgical needles for disease diagnoses and treatments [1,2]. During an insertion procedure, the needle punctures the skin and advances into the tissue. The mechanics of the needle insertion and extraction procedures are influenced by the needle design, material, geometry, and organ tissues [1-4]. During the insertion, it is known that the insertion force is significantly dominated by the friction force on the needle-tissue interface and the cutting force at the needle tip [1-4]. The insertion force is defined as the summation of the friction force and the cutting force; the extraction force depends only on the friction force. Since the insertion and extraction forces play a major role in tissue damage and target accuracy during percutaneous procedures, it is therefore critical to reduce these forces to improve the success of a procedure [5]. This work aims to reduce the insertion and extraction force by decreasing the friction force using a composite coating on surgical needles.

Medical researchers have explored the use of polymer and composite coatings on medical devices to decrease the friction force [6-13]. For example, coating of the surgical needle using silicone lubricants [7], diamond-like carbon coating on orthopedic implants [8], combination of diamond-like Carbon and parylene coating on Tuohy needles [9], the

metallic glass-coating on syringe needle [10]. In this work, a composite coating for surgical needles was developed by combining PDA for its strong adhesion properties with PTFE and activated Carbon (C) to create a low-friction coating. PDA has been commonly utilized as a thermal insulator and adhesive coating in needles, orthopedic implants, and drug delivery applications [11-14]. PDA can easily adhere to any organic and inorganic surfaces so it can be used as a medium of the adhesion between substrate and materials that are adhesion resistant. In addition to the adhesion properties, PDA has other beneficial properties such as biocompatibility and biodegradability, which are better suited for medical devices [12]. Previous studies also proved that the PDA could increase the durability and wear resistance of the composite material with the PDA used as the adhesion medium [11-14]. A coating material such as PTFE is also widely used in biomedical research because it has beneficial properties such as a low coefficient of friction, anti-microbial properties, hydrophobicity, biocompatibility, and chemical or drug resistance. However, PTFE has a non-stick property, which makes its coating less durable. Therefore, PDA can be used to overcome this non-adhesive shortcoming of the PTFE [13]. Additionally, the cured PTFE coating often experiences small creeps during the curing process, leading to small cracks and uneven surfaces [13,17]. In order to overcome this issue, an appropriate filler material needs to be added to minimize the cracks and uneven surfaces of the cured coating. In this

E-mail address: hutapea@temple.edu (P. Hutapea).

^{*} Corresponding author.

study, the activated Carbon powder with 250 microns grain size was utilized as a filler to reinforce PTFE surface cracks and uneven surfaces. [15]. Furthermore, the activated carbon particle also acts as a self-lubricant, providing low friction to the composite coating [16].

The current work investigates the effect of a composite coating comprised of PDA, PTFE, and activated Carbon on the insertion and extraction forces of needles advancing in tissues. The needle insertion and extraction procedures were conducted using a specially designed test setup. The tests were performed in PVC gel phantom and bovine kidney tissues to measure the insertion and extraction forces of uncoated and coated needles. Finally, Atomic Force Microscope (AFM) study was performed to evaluate the needle surface properties and to study the coating effect on the insertion and extraction forces.

2. Materials and methods

Three groups of needles were investigated in this study: (i) bare stainless-steel needles, (ii) stainless steel needles coated with PDA (basecoat) and PTFE (topcoat), and (iii) stainless steel needle coated with PDA (basecoat), and PTFE - C (topcoat). The steel biopsy needles used in this study had a diameter of 18 gauge (1.27mm) and a sharp trocar tip with a 0.2 cm tip length. As described in Figure 1, the PDA solution was prepared using dopamine hydrochloride and tris aminomethane [11-14]. Steel needles were first submerged into the PDA solution for 24 hours to grow the coating on the needle. Then, the needles were removed and rinsed with deionized water prior to the deposition of the PTFE. After rinsing the PDA-coated needles with deionized water, they were placed into the dip-coating machine fixture. The ready-made PTFE solution was placed in the dip-coating machine for coating the PDA-coated needles. The PDA coated needles were then dipped into the PTFE solution at the speed of 10 mm/min and kept for 3 min to form a thin PTFE layer on the PDA coated needles. Subsequently, the needles were extracted at a speed of 10 mm/min. Then, the PDA-PTFE coated needles were placed in the oven to dry at 120°C. Afterward, the needles were transferred to the furnace, where they were heated up to 373°C to remove water particles and the coating wetting agent [13,15,17]. As also shown in Figure 1, a similar coating procedure was used to create the PDA-PTFE-C coated needles, except that the PTFE was mixed with Carbon in Process 3. The coating process flow chart is shown in Figure 1.

As shown in Figure 2, a 3-Degree-of-Freedom (DOF) test setup

comprised of a linear actuator and a motor was fabricated and assembled. The combination of the linear actuator and the motor provided control of 3D needle maneuvering [18]. A 6 DOF F-T force sensor Nano17® (ATI Industrial Automation, Apex, NC) was attached to the needle fixture to measure the force exerted on the needle as it advanced in tissues. To study the effect of coating on multilayered isotropic tissue, initial experiments were performed on a two-layer PVC tissue phantom with a 15cm x 15cm x 3.5cm dimension. The top first layer had a 2 kPa of stiffness and a 2 cm of thickness, while the second layer had a 5 kPa of stiffness and a 1.5 cm of thickness. The two-layer tissue phantom was designed and manufactured to mimic the variation of tissue stiffness typically found in the bovine kidney. It was extremely challenging to imitate different tissues and veins of the bovine kidney; therefore, only two tissue cortex (2 kPa) and medulla (5 kPa) stiffness were manufactured for our experiments [19]. During an insertion and extraction cycle, the average insertion force is the summation of the friction and cutting forces from each layer, while the average extraction force is dependent on the friction force from each layer. So, the position of layers, whether placed on the top or the bottom, should not affect the measurement of the total forces. The same experimental procedure was also performed in bovine kidney tissue to see the effect of coating on the insertion and extraction forces.

Five insertions and extraction with each needle were performed during experiments. The test setup was configured to perform the insertion and extraction procedures at 5 mm/sec until the needle tip reached to the maximum insertion depth of 3.5 cm. The force sensor was programmed to start recording the force as soon as the needle touched the tissue. After each procedure, the needle traveled 2 cm horizontally over the tissue surface for the next insertion and extraction procedure. The recorded sets of data with a force sensor were acquired using a programmable LabVIEW data acquisition software.

To analyze the surface texture and the friction profile of needles, an AFM was utilized. The surface roughness of coated and uncoated needles was measured using the available contact mode method in the AFM. At least five randomly chosen areas were measured with the scan size of 30 microns for each different sample, and the roughness data were averaged [20]. The lateral force microscopy (LFM) method in AFM was used to measure the surface friction force between the needle interface and the AFM tip. The experiments were performed with a scan angle of 90° in a scan area of 30 microns. During the LFM measurement, one line was

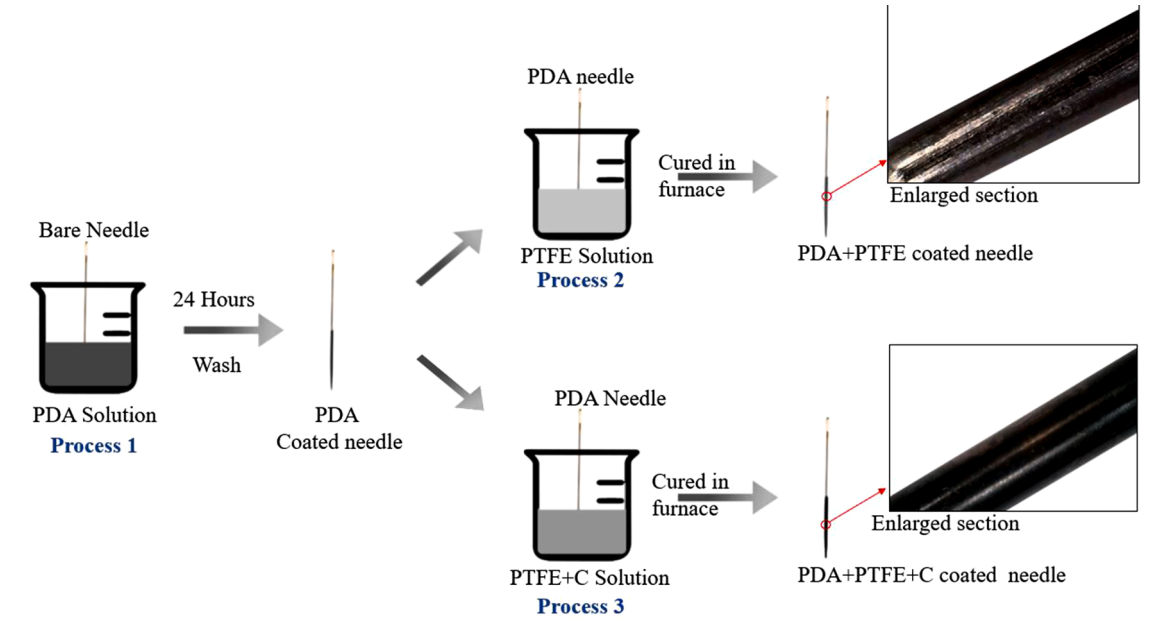


Fig. 1. (1) Process 1- Coating of the Bare needle with the Polydopamine; (2) Process 2 – Coating of PDA coated needle with the PTFE; (3) Process 3 – Coating of PDA coated needle with the PTFE and activated Carbon.

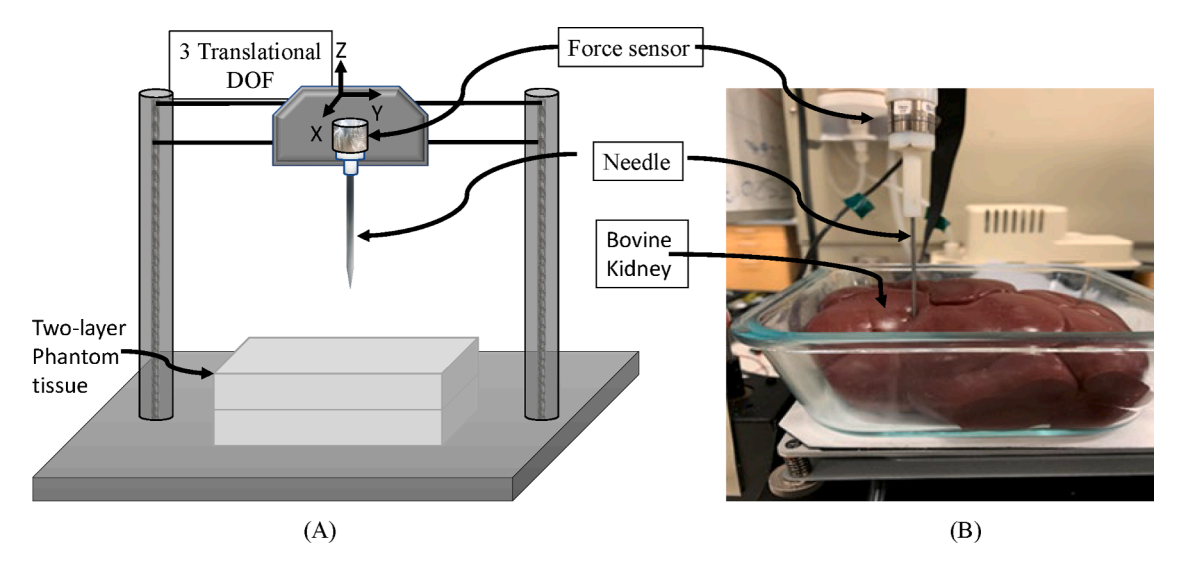


Fig. 2. (a) Test setup diagram for the two-layer phantom tissue: top layer (2 kPa, 2 cm thickness) and the bottom layer (5 kPa, 1.5 cm thickness). (b) Test setup for bovine kidney with the maximum height of 3.5 cm.

reciprocally scanned in the direction perpendicular to the cantilever beam (right direction), and one image was acquired by sequentially moving this measurement line in another direction (left direction). The right and left scanning directions of the images were named as trace and retrace, respectively. The images of the friction force profiles were treated by subtracting the trace scan image from the retrace scan images to enhance the friction force data. The tracking force during the scan was kept the same for all samples [21]. The friction force (f_f) can be calculated as $f_f = V.k.DS$, where V is the measured voltage, k is the spring constant, and DS is the calibrated deflection sensitivity [22].

3. Results and discussion

Figure 3(a) represents the average insertion and extraction forces generated on the insertion in the PVC tissue phantom. The upper region of the data shows the insertion force, and the lower region shows the extraction force. The insertion force is curvilinear because the two-layer PVC tissue phantom has isotropic properties with two different layers mimicking the bovine kidney. The needle tends to stick to the PVC tissue phantom during the extraction phase because the fabricated tissue phantom had a partial adherent property. The pressure of the tissue phantom and the partial adherent property would drag the tissue in an upward direction with the needle until the adherent bond is broken, which causes valleys during the extraction [23]. It is observed in Figure 3(a) that valleys are located at the absolute maximum point of the average extraction force. The average insertion and extraction forces associated with PDA-PTFE-C coated needles are calculated to be 62% and 64% lower than those of the uncoated needles. The results are repeatable as the calculated average standard deviation was 0.041 for the bare needle, 0.080 for PDA-PTFE coated needle, and 0.12 for PDA-PTFE-C coated needles upon the insertion in the PVC tissue phantom. Figure 3(b) shows the result of polymer-coated needle force data versus the depth for the experiment using bovine kidneys. The forces are nonlinear because the bovine kidney is anisotropic with tissues such as cortex, medulla, and non-homogeneous fibers distribution. The average insertion and extraction forces associated with PDA-PTFE-C coated samples are about 49% and 30% lower than those of the bare samples. Additionally, the average insertion and extraction forces for the PDA-PTFE-C needles were lower than those of the othercoated needles.

It can be determined that the results are reproducible because the average standard deviation is 0.052 for the bare needle, 0.048 for PDA-PTFE coated needle, and 0.023 for PDA-PTFE-C coated needles upon the insertion in the bovine kidney. A two-tailed statistical significance

method was performed with data to study the repetitiveness between data sets. The P-values for each comparison are less than $\alpha=0.05,$ proving that each data set has a null hypothesis. The maximum forces and the standard deviation data are tabulated in Table 1. From the results, the cutting force is shown to be very small compared to the friction force; therefore, the needle insertion force graphs do not exhibit any significant initial spike when the sharp trocar tip needle fractures the tissue.

AFM was used to analyze the surface roughness of needles. After the AFM analysis, the surface roughness root mean square (Rq) value for PDA-PTFE-C coated needle was around 218 nm, and it was 160.48 nm for the bare needle. The AFM images of the bare needle and the PDA-PTFE coated needle have a random surface texture profile, as shown in Figures 4(a) and 4(b). In contrast, the PDA-PTFE-C coated needle has a unidirectional surface profile with some waviness in it, as shown in Figure 4(c).

The friction force between the AFM tip and needles was measured using the LFM technique with a scan angle of 90° and a scan area of 30 micros. The friction force image profiles were obtained by subtracting the trace scan image from the retrace scan images. The LFM friction profile and line profile of the needles are shown in Figure 5.

The maximum average friction force between the needle and AFM tip of the PDA-PTFE-C coated needle is 23.9 nN, while the bare needle friction force is 69.7 nN. The friction force between the needle surface and the AFM tip; and the surface roughness values are tabulated in Table 2. It can be determined that the maximum friction force of the PDA-PTFE-C coated needle is decreased by 65.7% compared to the bare needle.

When the needle tip entered the tissue, the average forces for all tested needles remained between 0.05 to 0.12 N for the initial 0.2 cm insertion depth (i.e., the tip length of the needle), as shown in Figure 3. Therefore, the average insertion force for the first 0.2 cm insertion depth was the cutting force. The contact area between the needle and tissue increased as the needle advanced in-depth; therefore, the friction became increasingly dominant over the cutting force. So, the cutting force is small compared to the friction force at the maximum depth of 3.5 cm. The cutting force depends on the needle geometry [26]. It remains constant throughout the insertion depth in isotropic tissues but marginally changes in anisotropic tissues [1,2].

From Table 1, the average insertion and extraction forces decreased in a PDA-PTFE-C coated needle compared to the bare needles and the PDA-PTFE coated needles. It was already well known that the friction force was the main contributor to the insertion and extraction forces.

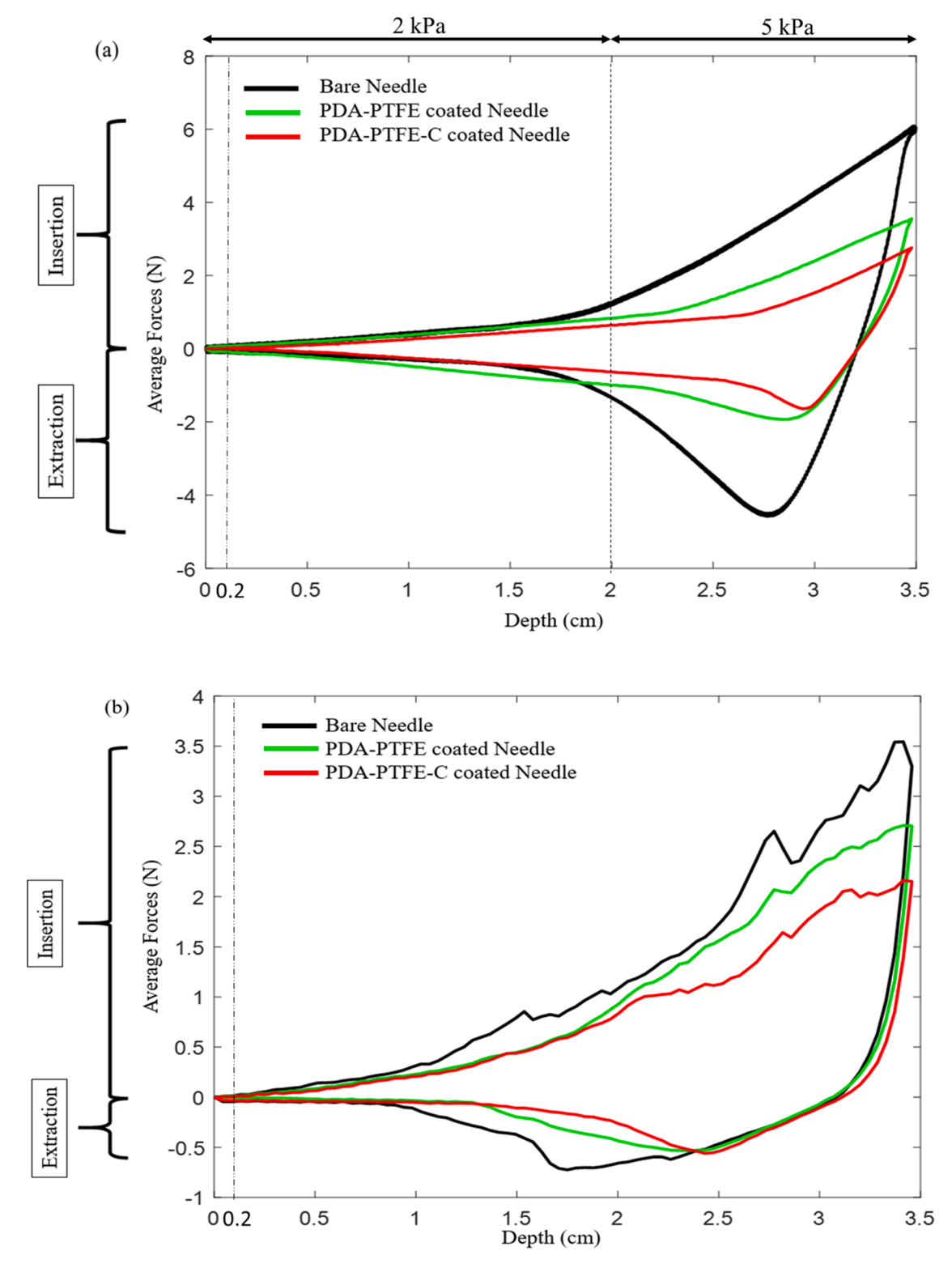


Fig. 3. Force profiles for bare needle, PDA-PTFE coated needle, and PDA-PTFE-C coated needle in (a) PVC tissue phantom, and (b) bovine kidney.

However, at this point, it was almost impossible to measure the friction force on the needle and tissue interface without existing sensor technologies. Therefore, the AFM was used to study the effect of the coating on the friction force between the needle surface and the AFM probe tip. It can be conjectured that if the friction force is reduced as in this case, it should also be reduced if the needle is inserted into tissues. The friction force measured with the AFM test for the PDA-PTFE-C coated needle was reduced by 65.7% compared to those of the bare and PDA-PTFE coated

needles.

From Table 2, it was observed that although the PDA-PTFE-C coated needles had larger surface roughness R_q , lower friction and insertion forces. This transpired because the friction not only depends on the surface roughness but also depends on the material mechanical properties, the surface texture (roughness, waviness, and the characteristics of lay), the mutual dissolution of materials, the contact time, partial adherence (stickiness), and the lubricant film properties [24,25,27]. The

 Table 1

 Average maximum forces of different needles.

| Coating Material | Average Maximum Insertion Force, (N) | | Average Maximum Extraction Force, (N) | |
|---------------------|---|------------------|--|------------------------------------|
| | Phantom Tissue | Bovine Kidney | Phantom Tissue | Bovine Kidney |
| Bare | 6.02 ± 0.04 | 3.54 ± 0.05 | -4.58 ± 0.04 | $\textbf{-0.72} \pm \textbf{0.05}$ |
| PDA-PTFE | 3.37 ± 0.08 | 2.71 ± 0.05 | $\textbf{-1.93} \pm 0.08$ | $\textbf{-0.68} \pm 0.05$ |
| PDA-PTFE-C | 2.27 ± 0.12 | $1.82~\pm$ | $\textbf{-1.64} \pm 0.12$ | $\textbf{-0.50} \pm 0.02$ |
| | | 0.023 | | |

PDA-PTFE-C coating shows significant reductions in the insertion and extraction forces because of PTFE non-stick properties, activated Carbon filler and self-lubrication properties, and unidirectional surface texture.

4. Conclusion

It was hypothesized that the PDA-PTFE-C coating on the needle decreases the average insertion and extraction forces. The results support the hypothesis as they show that the addition of activated Carbon particles in the PDA-PTFE films significantly decreased the average insertion and extraction forces by 62% and 64%, respectively, when tested in PVC tissue phantom and by 49% and 30%, respectively, in bovine

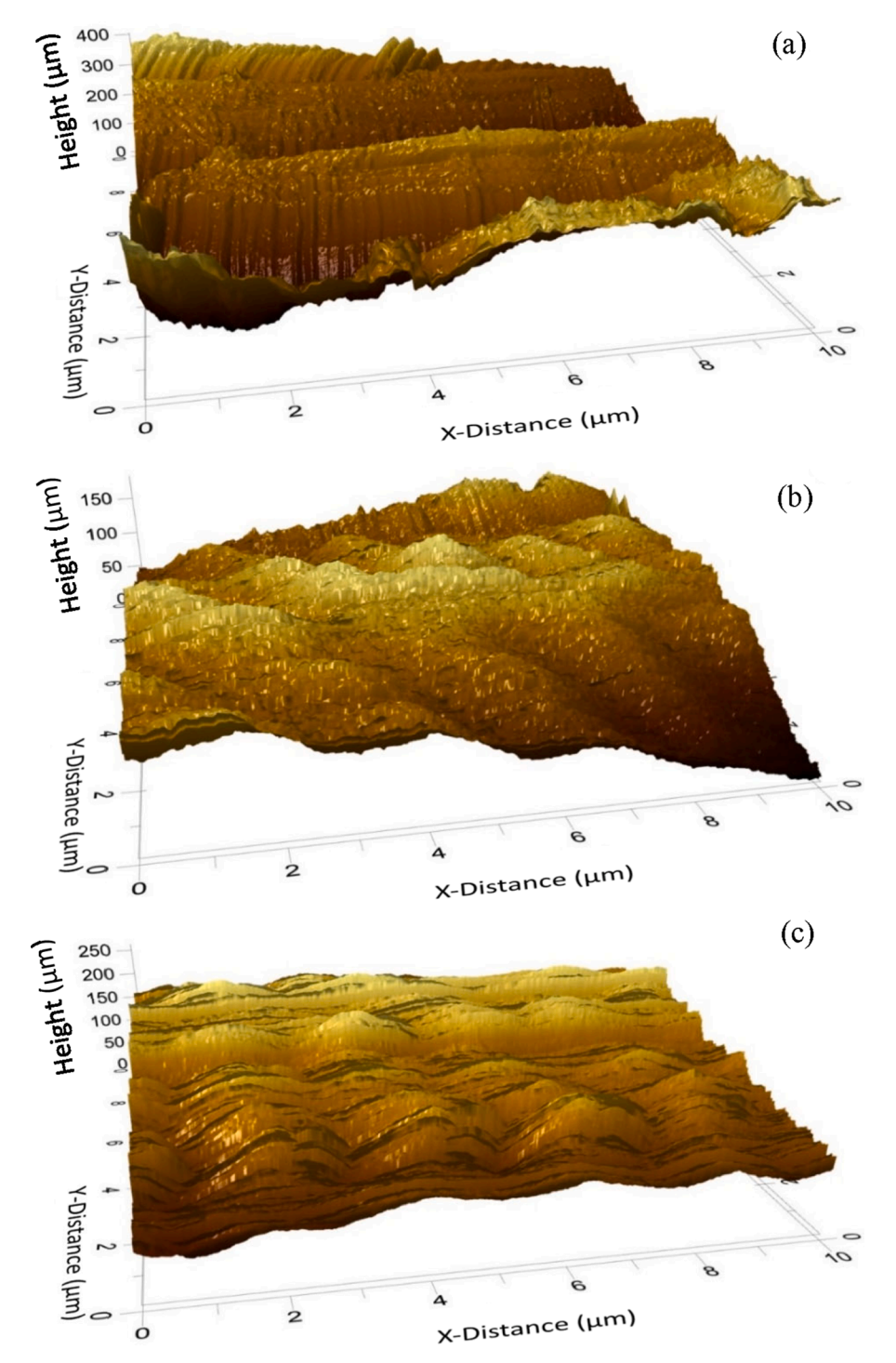


Fig. 4. (a) AFM topography of bare needle (b) AFM topography of PDA-PTFE coated needle (c) AFM topography of PDA-PTFE-C coated needle.

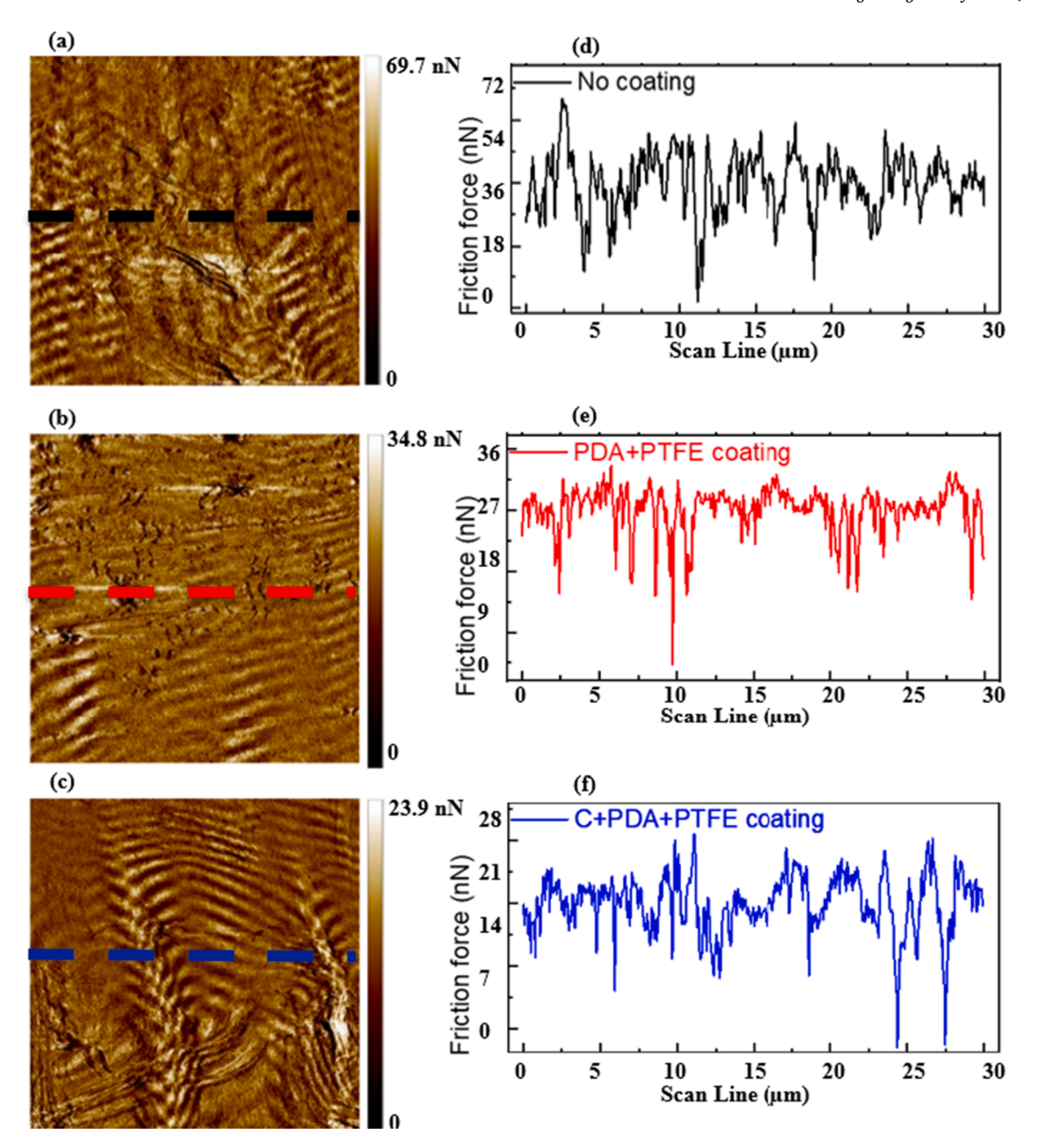


Fig. 5. LFM friction profile of (a) bare needle (b) PDA-PTFE coated needle (c) PDA-PTFE-C coated needle; Cross-sectional friction line profile of (d) the bare needle (e) PDA-PTFE coated needle (f) PDA-PTFE-C coated needle. Scan size: 30 µm.

Table 2 Surface roughness $R_{\rm q}$ (nm) and friction force recorded by the AFM.

| Coating Material | Surface Roughness RMS R_q (nm) | Maximum Average Friction Force between AFM tip and Needles (nN) |
|---------------------|----------------------------------|--|
| Bare | 160.48 | 69.7 |
| PDA-PTFE | 94.00 | 34.8 |
| PDA-PTFE-C | 218.12 | 23.9 |

kidney tissue. It is concluded that this is due to the non-stick, self-lubricating coating property and the unidirectional surface texture with the waviness of the composite coating observed in the AFM study. Delamination of the coating was not observed visually either on PVC phantom or bovine kidney during experiments. Detailed studies of durability, biocompatibility, coefficient of friction, sterilization, and tissue damage are ongoing. It can be concluded that the composite coating of PDA-PTFE-C significantly decreased the insertion and

extraction forces, which could improve the performance of surgical needles during percutaneous procedures.

Declaration of Competing Interest

None Declared.

Acknowledgments

The authors would like to acknowledge National Science Foundation (CMMI Award #1917711) for the financial support.

Funding

National Science Foundation CMMI Award #1917711

Ethical approval

Not required.

References

- Okamura AM, Simone C, O'Leary MD. Force modeling for needle insertion into soft tissue. IEEE Trans Biomed Eng 2004;51:1707–16. https://doi.org/10.1109/ TBME.2004.831542. https://doi.org/.
- [2] Cheng Z, Chauhan M, Davies BL, Caldwell DG, Mattos LS. Modeling needle forces during insertion into soft tissue. In: Proceedings of the Annual International Conference of the IEEE Engineering in Medicine and Biology Society. EMBS; 2015. https://doi.org/10.1109/EMBC.2015.7319477. https://doi.org/.
- [3] Sahlabadi M, Khodaei S, Jezler K, Hutapea P. Insertion mechanics of bioinspired needles into soft tissues. Minimal Invas Thera Allied Tech 2018;27. https://doi. org/10.1080/13645706.2017.1418753. https://doi.org/.
- [4] Sahlabadi M, Hutapea P. Novel design of honeybee-inspired needles for the percutaneous procedure. Bioinspiration and Biomimetics 2018;13:036013. https://doi.org/10.1088/1748-3190/aaa348. https://doi.org/.
- [5] Sahlabadi M, Hutapea P. Tissue deformation and insertion force of bee-stinger inspired surgical needles. J Med Dev Trans ASME 2018;12. https://doi.org/ 10.1115/1.4040637. https://doi.org/.
- [6] Ching HA, Choudhury D, Nine MJ, Abu Osman NA. Effects of surface coating on reducing friction and wear of orthopedic implants. Sci Technol Adv Mater 2014;15. https://doi.org/10.1088/1468-6996/15/1/014402. https://doi.org/.
- [7] McClung W. Enhancing needle durability by silicone coating of surgical needles.
 J Emerg Med 1995;13(4):515–8. https://doi.org/10.1016/0736-4679(95)00035-9. https://doi.org/.
- [8] Dearnaley G, Arps JH. Biomedical applications of diamond-like carbon (DLC) coatings: A review. Surf Coat Technol 2005;200(7):2518–24. https://doi.org/10.1016/j.surfcoat.2005.07.077. https://doi.org/.
- [9] Doerzbacher M, Barnett A, Brandmeir N, Wolfe D, Zheng S, Moore J. Advanced needle coatings for improved lumbar drain procedure. J Med Dev Trans ASME 2013;7. https://doi.org/10.1115/1.4024485. https://doi.org/.
- [10] Chu JP, Jang JSC, Huang JC, Chou HS, Yang Y, Ye JC, et al. Thin film metallic glasses: Unique properties and potential applications. Thin Solid Films 2012;520: 5097–122. https://doi.org/10.1016/j.tsf.2012.03.092. https://doi.org/.
- [11] Foust SA. Ultrathin PTFE Coating for Hypodermic Needles Enabled by Mussel-Inspired PDA Adhesive Laver 2014.
- [12] Crisp DJ, Walker G, Young GA, Yule AB. Adhesion and substrate choice in mussels and barnacles. J Colloid Interface Sci 1985;104:40–50. https://doi.org/10.1016/ 0021-9797(85)90007-4. https://doi.org/.
- [13] Beckford S, Mathurin L, Chen J, Fleming RA, Zou M. The effects of polydopamine coated Cu nanoparticles on the tribological properties of polydopamine/PTFE

- coatings. Tribol Int 2016;103:87–94. https://doi.org/10.1016/j.triboint.2016.06.031. https://doi.org/.
- [14] Sahlabadi M, Zhao Y, Jezler K, Gardell D, Lee HH, Ren F, Hutapea P. Polydopamine coating for thermal insulation of shape memory alloy wires. In: ASME 2016 Conference on Smart Materials, Adaptive Structures and Intelligent Systems. SMASIS; 2016. p. 1. https://doi.org/10.1115/SMASIS2016-9265. https://doi.org/.
- [15] Nor NA, Mohamed M, Mohamad M, Amini MHM, Abdul Aziz MS, Yusoff H, et al. Influence of activated Carbon filler on the mechanical properties of wood composites. ARPN J Eng Appl Sci 2015:10.
- [16] Baik S, Yoon D, Lee HI, Ji MK, Gyu-Sun L, Young-Ze L. Frictional performances of activated carbon and carbon blacks as lubricant additives. Tribol Trans 2009;52: 133–7. https://doi.org/10.1080/10402000802192693. https://doi.org/.
- [17] Khoddamzadeh A, Liu R, Wu X. Novel polytetrafluoroethylene (PTFE) composites with newly developed Tribaloy alloy additive for sliding bearings. Wear 2009;266: 646–57. https://doi.org/10.1016/j.wear.2008.08.007. https://doi.org/.
- [18] Patel KI, Gidde STR, Li H, Podder T, Ren F, Hutapea P. Insertion force of polydopamine-coated needle on phantom tissues. In: Frontiers in Biomedical Devices, BIOMED-2019 Design of Medical Devices Conference, DMD; 2019. https://doi.org/10.1115/DMD2019-3271. https://doi.org/.
- [19] Egorov V, Tsyuryupa S, Kanilo S, Kogit M, Sarvazyan A. Soft tissue elastometer. Med Eng Phys 2008;30. https://doi.org/10.1016/j.medengphy.2007.02.007. https://doi.org/.
- [20] Yang C-W, Leung K, Ding R-F, Ko H-C, Lu Y-H. Lateral Force Microscopy of Interfacial Nanobubbles: Friction Reduction and Novel Frictional Behavior. OPEN 2018;8:3125. https://doi.org/10.1038/s41598-018-21264-6. https://doi.org/.
- [21] Tsuchiko M, Aoki S. in-Liquid Lateral force Microscopy of Micropatterned Surfaces in a fatty Acid Solution under Boundary Lubrication 2019; 9:15236. https://doi. org/10.1038/s41598-019-51687-8.
- [22] Nagy ÁG, Kámán J, Horváth R, Bonyár A. spring constant and sensitivity calibration of FluidFM micropipette cantilevers for force spectroscopy measurements 2019; 9:10287 https://doi.org/10.1038/s41598-019-46691-x.
- [23] Chu JP, Yu CC, Tanatsugu Y, Yasuzawa M, Shen YL. Non-stick syringe needles: Beneficial effects of thin film metallic glass coating. Sci Rep 2016. https://doi.org/ 10.1038/srep31847. https://doi.org/.
- [24] Branko Ivkovic, Durdanovic Miroslav SD. The influence of the contact surface roughness on the static friction coefficient. Tribol Indust 2000;22:41–4.
- [25] Menezes PL, Kailas SV. Role of surface texture and roughness parameters on friction and transfer film formation when UHMWPE sliding against steel. Biosurf Biotribol 2016;2:1–10. https://doi.org/10.1016/j.bsbt.2016.02.001. https://doi. org/.
- [26] Chebolu A, Mallimoggala A, Nagahanumaiah. Modelling of Cutting Force and Deflection of Medical Needles with Different Tip Geometries. Procedia Mater Sci 2014;5. https://doi.org/10.1016/j.mspro.2014.07.535. https://doi.org/.
- [27] Zhou Y, Zhu H, Zhang W, Zuo X, Li Y, Yang J. Influence of surface roughness on the friction property of textured surface. Adv Mech Eng 2015;7. https://doi.org/10.1177/1687814014568500. https://doi.org/